Supplement of Weather Clim. Dynam., 2, 777–794, 2021
https://doi.org/10.5194/wcd-2-777-2021-supplement

Supplement of

Reconstructing winter climate anomalies in the Euro-Atlantic sector using circulation patterns

Erica Madonna et al.

Correspondence to: Erica Madonna (erica.madonna@uib.no)

Supplementary Material

Supplementary Material

A) Sensitivity analysis to the choice of the parameter d (Figs. A1-A4)

B) Supplementary Figures:

- Figure S1: Zonal wind, precipitation, and temperature anomalies for the undefined categories (NAO, blocking, and jet).
- Figure S2: Reconstructed anomalies ($\overline{p}$) for zonal wind, precipitation, and temperature for the NAO, blocking, and jet.
- Figure S3: Correlation coefficient for precipitation, temperature, and wind for the NAO, blocking, and jet.
- Figure S4: Standard deviation of winter precipitation, and temperature for ERA-Interim (1979-2014).
- Figure S5: Coefficient of efficiency for precipitation, temperature, and wind for the NAO, blocking, and jet.
- Figure S6: Correlation between reconstructed and observed winter precipitation anomalies averaged over northern and southern Europe for the different classification methods.
- Figure S7: Composite mean precipitation, standard deviation, and their ratio for different classes.
- Figure S8: Composite mean temperature, standard deviation, and their ratio for different classes.

References

Fereday, D., Chadwick, R., Knight, J., and Scaife, A. A. : Atmospheric dynamics is the largest source of uncertainty in future winter European rainfall, J. Climate, 31, 963-977, 2018.

A Sensitivity Analysis

We perform a sensitivity analysis to investigate the effect of the threshold applied to the inverse distance from the cluster centroid (d) to defined the five jet clusters (cf. Section 2.1.3). Four different thresholds of the inverse Euclidean distance d are used to identify the five jet clusters, namely d=0.5 (the original threshold), d=0.4, d=0.3 and d=0 (i.e. no restriction, all days are defined and belong to one of the five clusters). The mean number of undefined days per winter depending on the chosen threshold are 41.4, 20.8, 3.0, and 0, respectively.

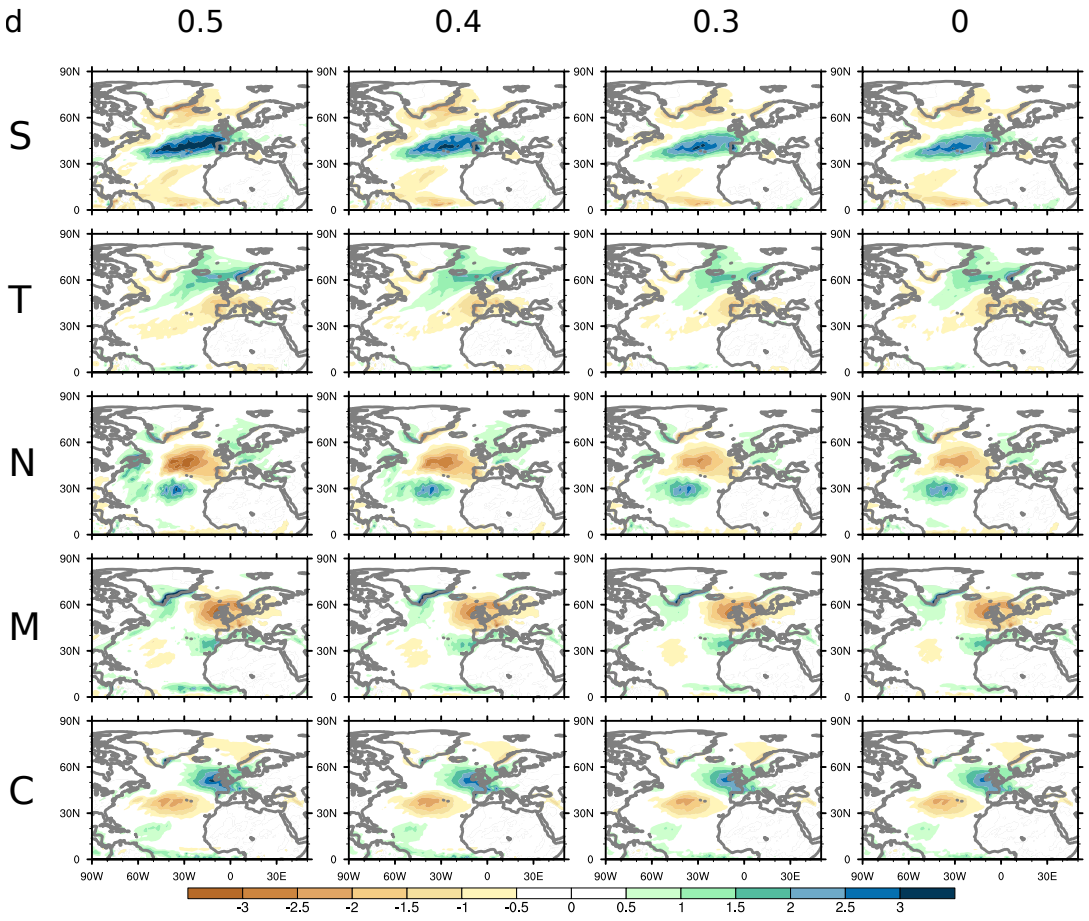

Figure A1. Composites of precipitation anomalies (in mm day^{-1}) for S-jet, T-jet, N-jet, M-jet, and C-jet, depending on the threshold d (0.5, 0.4, 0.3, 0).

Figure A1 shows for precipitation the changes in the composite anomaly patterns depending on the chosen threshold. The anomalies become slightly weaker with decreasing d (i.e. by including more days in the composites), but the patterns remain very similar. Similar conclusions can be drawn for zonal wind and temperature (not shown).

After calculating for each threshold the mean temperature and anomaly patterns, we proceed as described in the paper, i.e. calculate the winter time series of the occurrence of each cluster, reconstruct the seasonal anomalies, calculate the coefficient of efficiency (CE), and the scaling factor (β).

Figure A2 shows the time series of the number of days in each cluster for different d. As expected, lowering the threshold increases the number of days per winter that belong to each cluster. The time series for each cluster are highly correlated with each other.

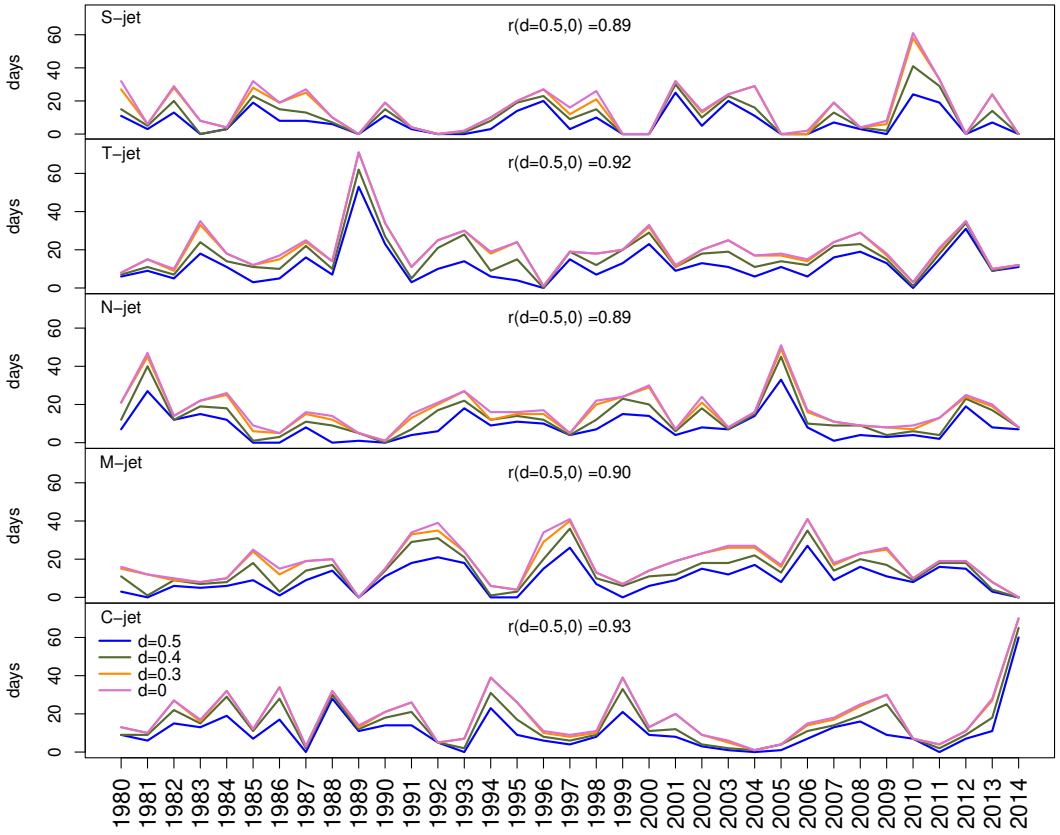

Figure A2. Time series of the number of days per winter of S-jet, T-jet, N-jet, M-jet, and C-jet, depending on the threshold d (colour legend, 0.5, 0.4, 0.3, 0). Correlations r between d =0.5 and d =0 (no restriction) are shown at the top of each panel.

The CE is calculated using Equation 3 of the manuscript for d =0.5, 0.4, 0.3, and 0 (no restrictions) and shown for zonal wind, precipitation, and temperature in Figure A3. These values represent the "raw" data, i.e. no scaling factor has been applied (similar to Figure 7).

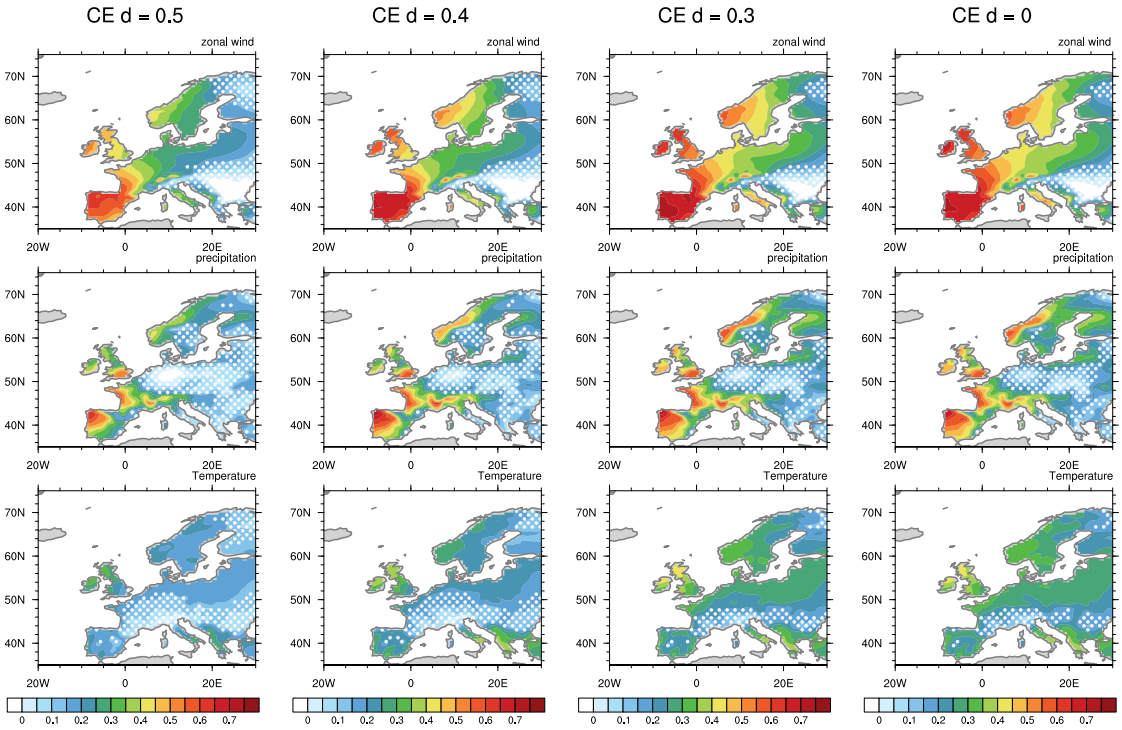

Figure A3. CE (unscaled) for wind, precipitation, and temperature for reconstructions using 5 jet clusters with different thresholds d (0.5, 0.4, 0.3, 0). White dots mark regions with correlation between the observed and reconstructed variables below 0.5.

The general patterns are similar, and we observe a slight increase in CE with decreasing d. The CE for temperature shows a better reconstruction over most of central and northern Europe using all days (d =0) compared to d =0.5.

We calculate the scaling factor (β) that maximises CE for the different thresholds (Table S1). The underestimation in the amplitude of the reconstruction, represented by the scaling factor, is lower when more days are used for the reconstruction (lower d). When using all days (d =0), we still have scaling factors of 1.5, 1.6, and 1.9 for wind, precipitation, and temperature, respectively.

To summarize, using more days to reconstruct climate anomalies improves the overall skill slightly, but does not lead to improvement of reconstructions in regions that had previously very poor skill (i.e. the CE patterns are quite similar). The representation of the amplitude of the seasonal anomalies improves with decreasing d as well. Even when using all days we do not achieve perfect reconstructions ($\beta > 1$).

Table S1. Scaling factors β for five jet clusters as a function of d for gridpoints over Europe (only land) and only with correlation larger than 0.5.

scaling factor β	precipitation	temperatures	zonal wind
$d = 0.5$	1.8	2.2	1.7
$d = 0.4$	1.6	2.0	1.5
$d = 0.3$	1.6	1.9	1.5
$d = 0$	1.6	1.9	1.5

Finally, in order to assess the effect of internal variability on the calculation of the CE, the reconstructions of the seasonal anomalies are re-calculated 100 times using different combinations (bootstrap with replacement) of 35 years of the original time series (i.e. pairs of observations and reconstructions). Figure A4 shows for $d = 0.5$ that the CE changes only marginally.

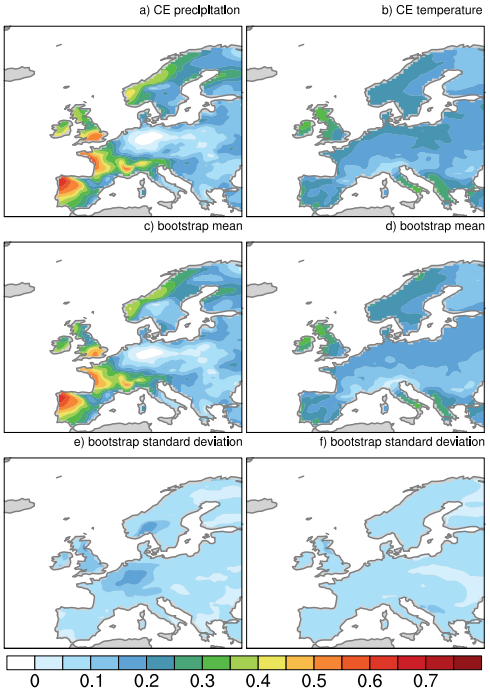

Figure A4. Coefficient of efficiency (CE) for Europe for (a) precipitation and (b) temperature for five jet clusters and $d = 0.5$, as in Figure 7e,f. (c-d) Mean CE for (left) precipitation and (right) temperature calculated from a 100 bootstrap samples of 35 seasons with replacement. (e-f) Standard deviation of CE for the 100 bootstrapped samples.

B Supplementary Figures

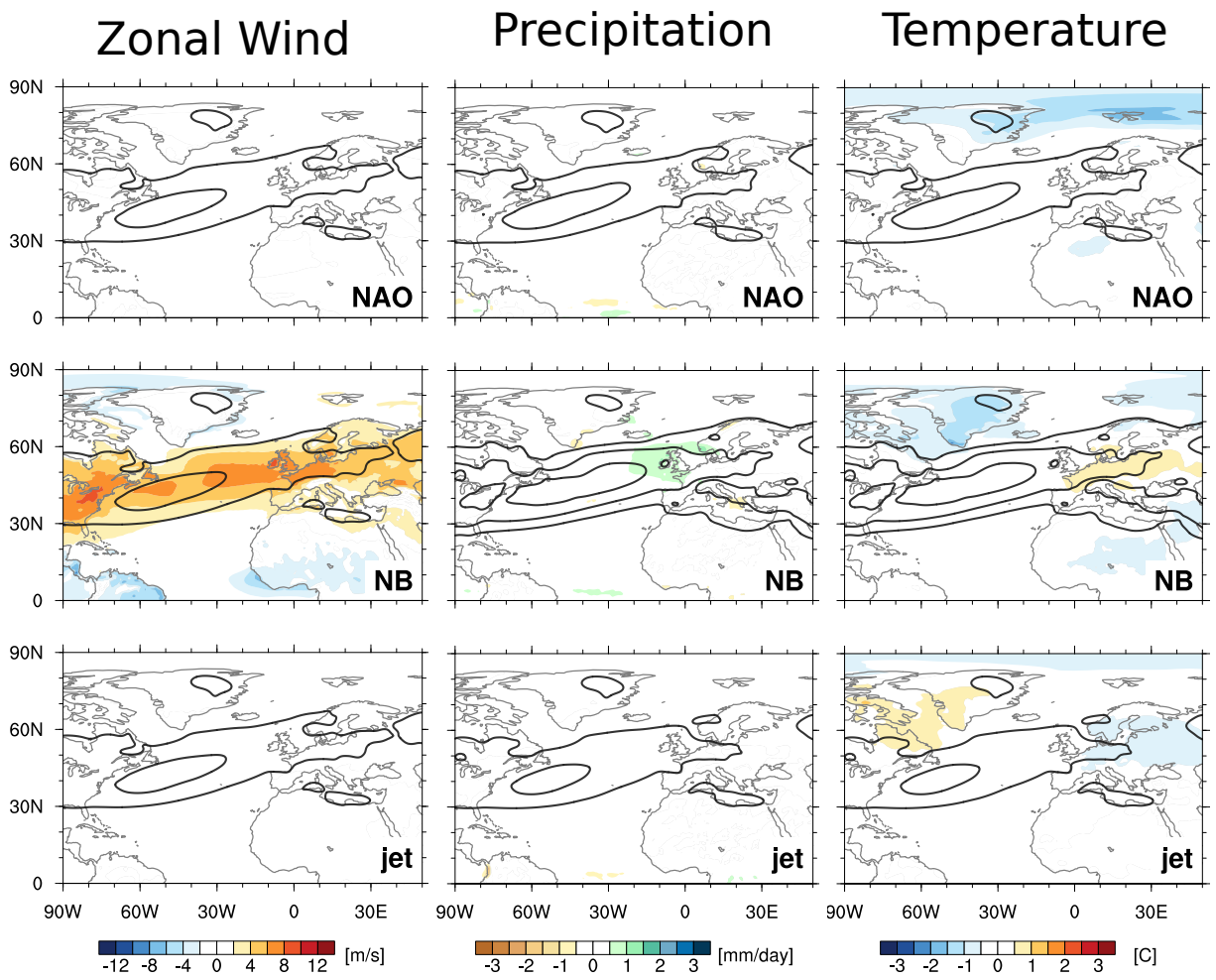

Figure S1. Zonal wind anomalies at 850 hPa (shading, in m s^{-1}), precipitation anomalies (shading, in mm day^{-1}), and temperature anomalies (shading, in °C) for (1st row) NAO neutral days, (2nd row) non-blocked (NB) days, and (3rd row) undefined jet days. Black contours show the zonal wind (interval, 5 m s^{-1}) climatology (for the wind column) and the composite wind for the precipitation and temperature columns, as in Figure 2-4.

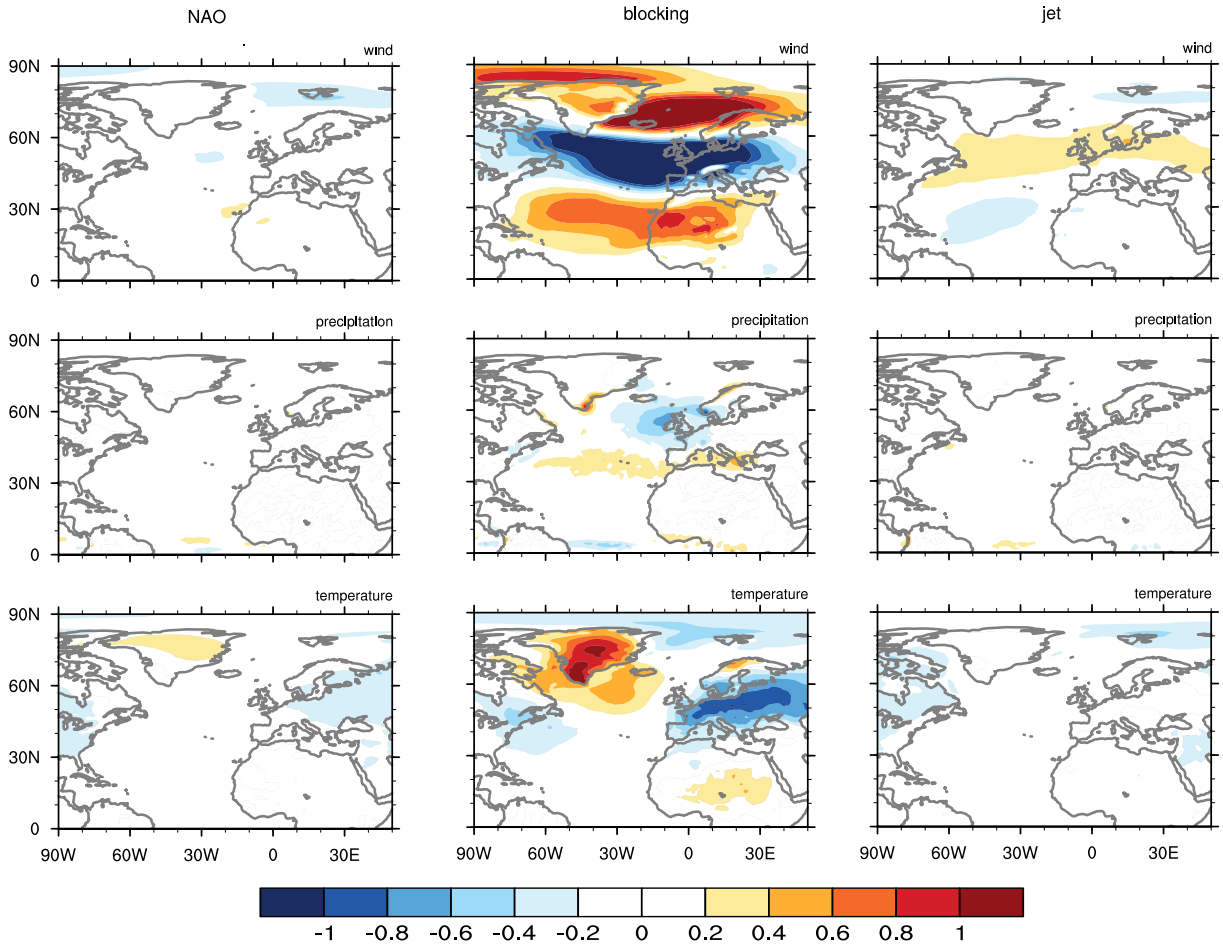

Figure S2. Mean of reconstructed anomalies ($\overline{p}$) for (1st row) zonal wind (in $\mathrm{m\,s^{-1}}$), (2nd row) precipitation (in $\mathrm{mm\,day^{-1}}$), and (3rd row) temperature (in $^{\circ}$C) for the NAO, blocking, and jet classifications. Anomalies are close to zero for the reconstructions using the NAO and the jet, while deviations from zero are observed for reconstructions using blocking.

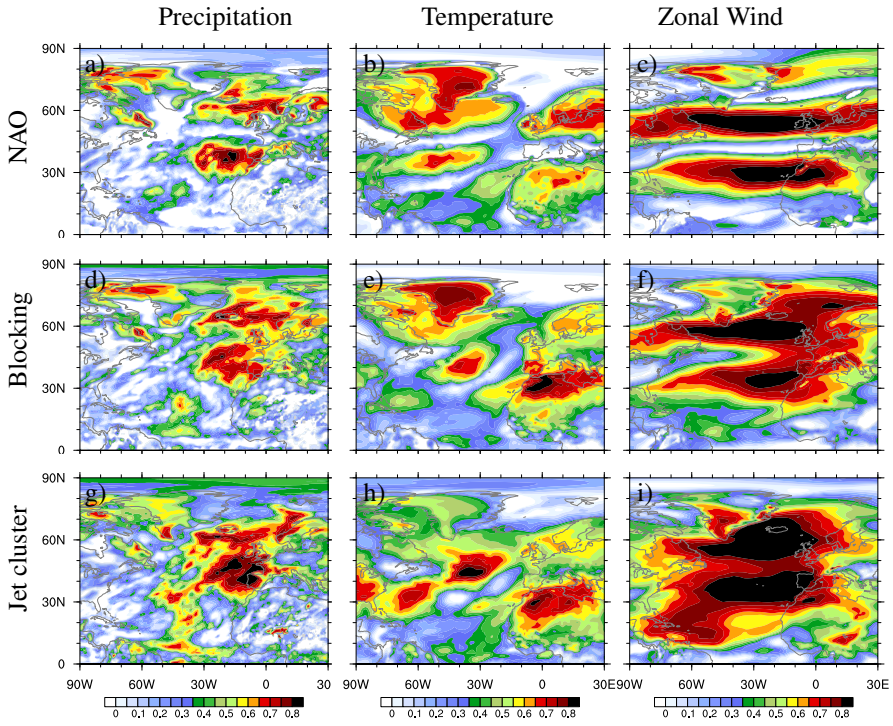

Figure S3. Similar to Figure 6, correlation between reconstructed and observed precipitation, temperature, and zonal wind over a larger domain for two NAO phases (a-c), three blocking categories (d-f) and five jet clusters (g-i).

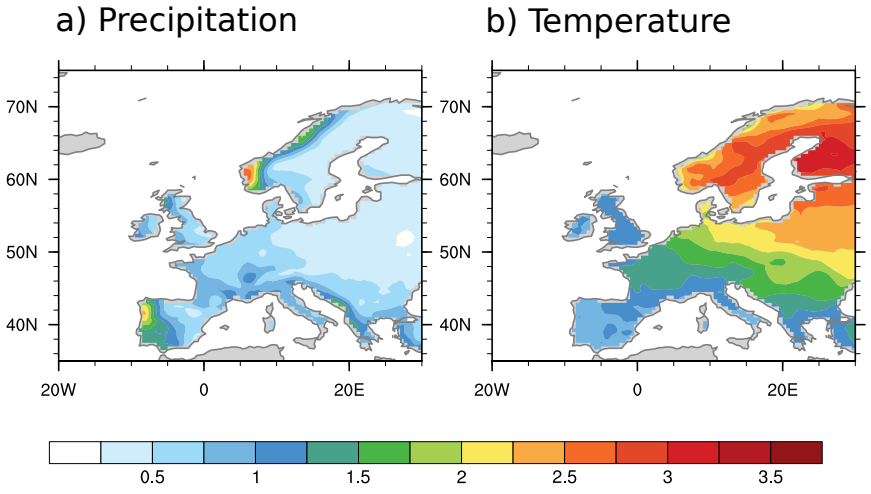

Figure S4. Standard deviation of (a) precipitation (in mm day^{-1}) and (b) temperature (in °C) over 35 ERA-Interim winter means.

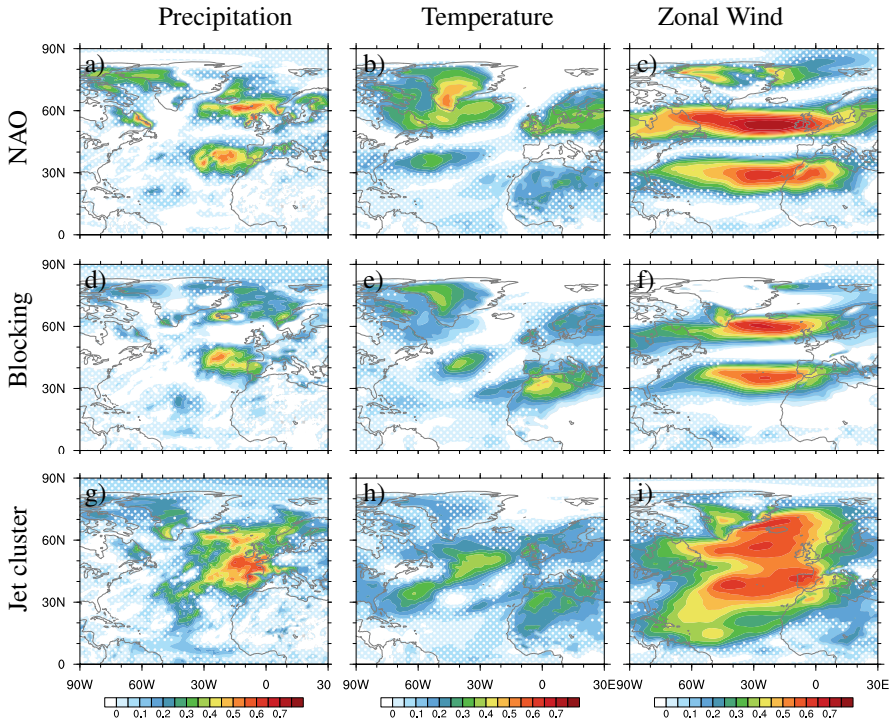

Figure S5. Similar to Figure 7, CE for precipitation, temperature, and zonal wind over a larger domain for two NAO phases (a-c), three blocking categories (d-f) and five jet clusters (g-i). White dots mark regions with correlation below 0.5.

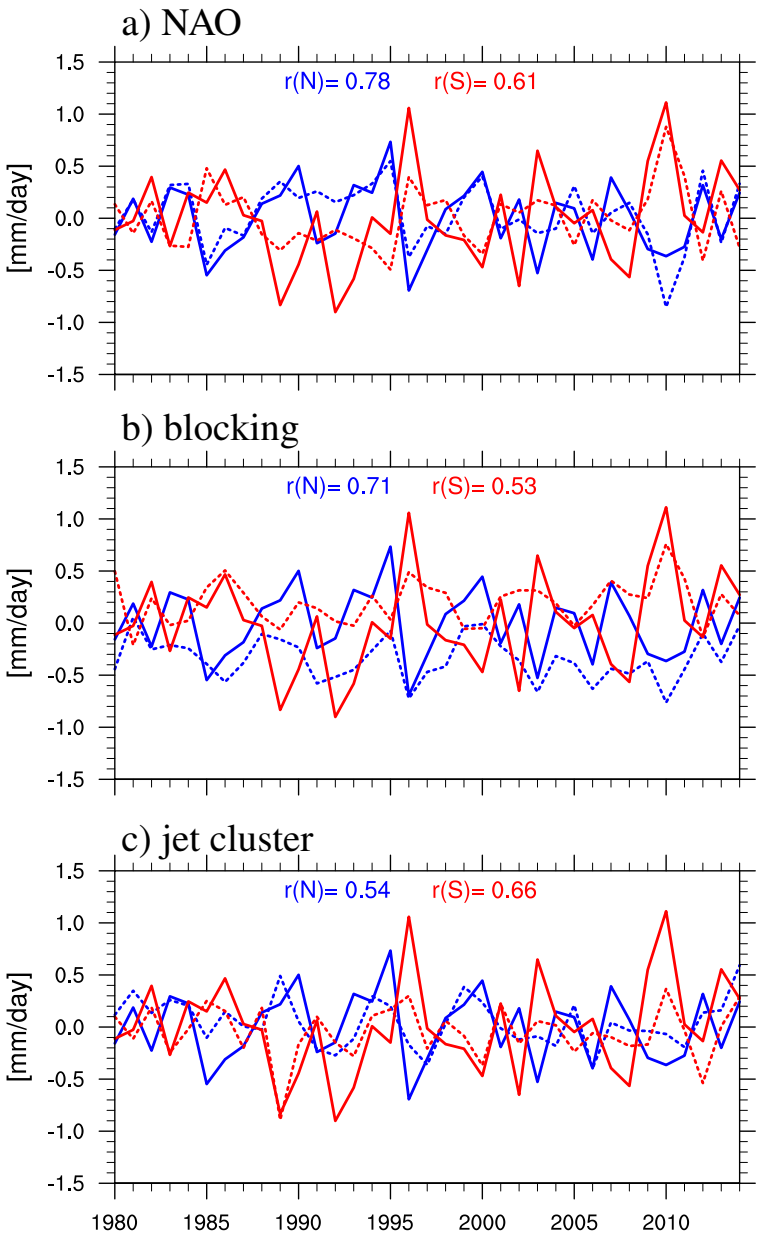

Figure S6. Mean winter precipitation anomalies for northern (N, blue) and southern (S, red) Europe from ERA-Interim (solid) and the reconstructions (dashed) using two NAO phases (a), three blocking categories (b), and five jet clusters (c). Northern Europe is defined as 48-75°N, 10°W-30°E, southern Europe as 35-48°N, 10°W-30°E, following Fereday (2018). Correlation values r between reanalysis and reconstructions for the two regions are shown in each panel.

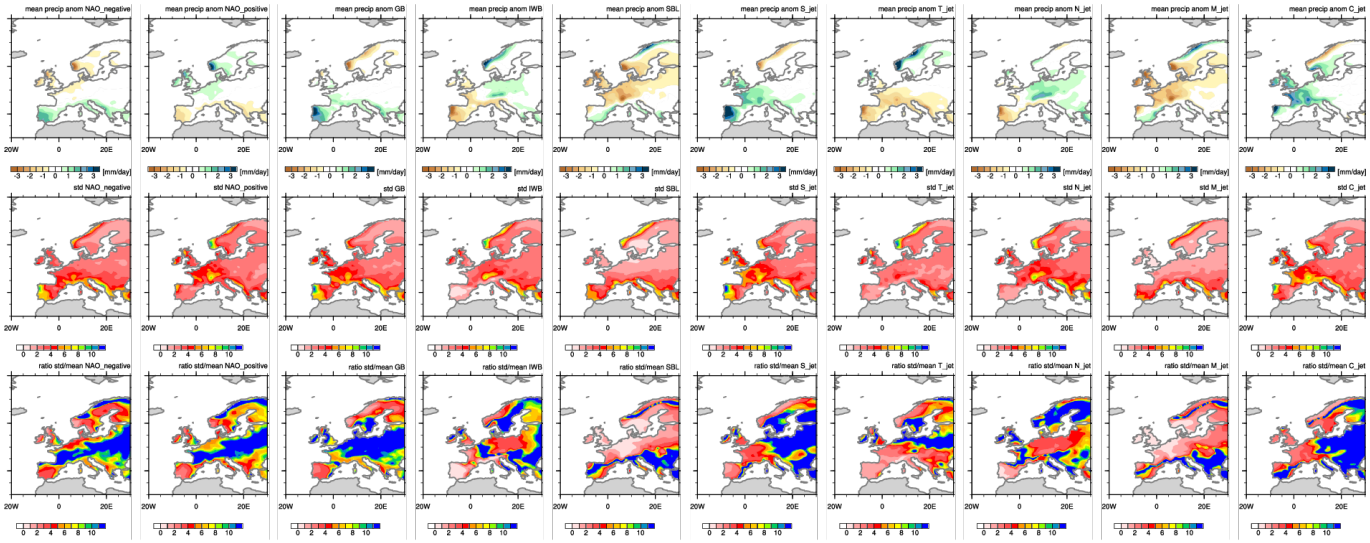

Figure S7. Precipitation (1st row) anomalies (in mm day^{-1}), (2nd row) standard deviation (in mm day^{-1}), and (3rd row) their ratio (anomalies/std) for NAO positive, NAO negative, GB, IWB, SBL, S-jet, T-jet, N-jet, M-jet, and C-jet.

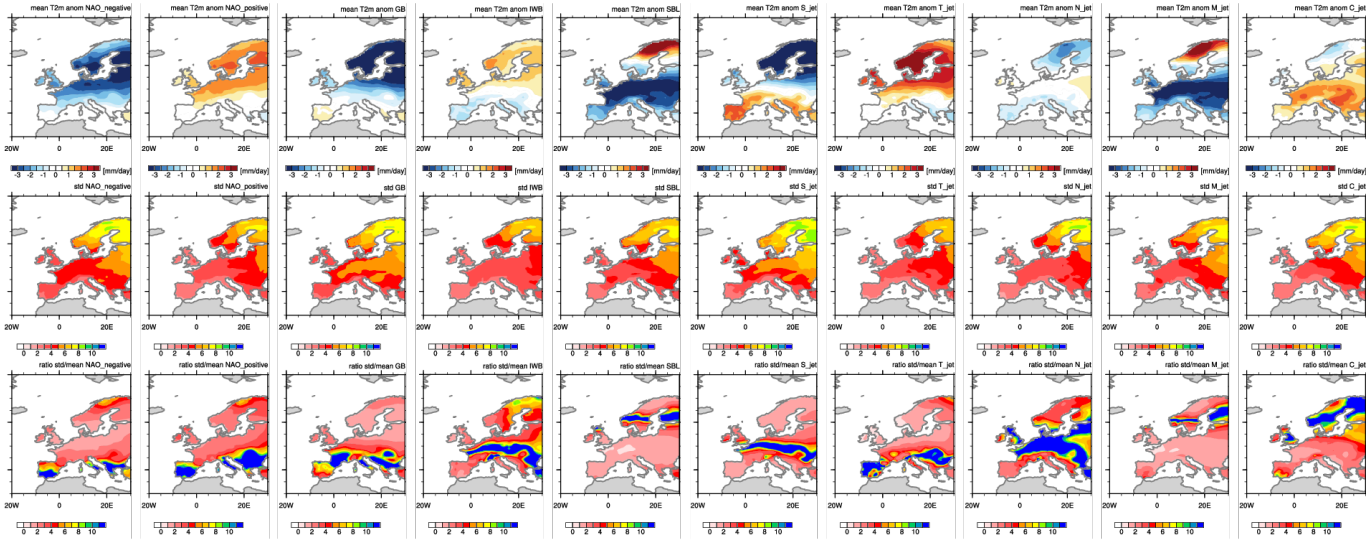

Figure S8. Same as Figure S7 but for temperature (in °C).